Electronic Supplementary Material (ESI) for CrystEngComm

Supporting Information

Synthesis and Shape-dependent Catalytic Properties of CeO_2 Nanocubes and Truncated Octahedra†

Xue Wang, Zhiyuan Jiang,* Binjie Zheng, Zhaoxiong Xie,* and Lansun Zheng

State Key Laboratory of Physical Chemistry of Solid Surfaces & Department of Chemistry, College of Chemistry and Chemical Engineering, Xiamen University, Xiamen 361005, China

E-mail: zyjiang@xmu.edu.cn, zxxie@xmu.edu.cn

Experimental Section

1. Regents: $Ce(NO_3)_3{\cdot}6H_2O$, 1.00 M tetramethylammonium hydroxide (TMAH) aqueous solution, oleic acid, Polyvinyl pyrrolidone (PVP, K-30) were purchased from commercial suppliers (Alfa Aesar and Sinopharm Chemical Regent Co., Ltd.) and used as received without further purification.

2. Synthetic methods.

2.1. Synthesis of cubic CeO_2 enclosed by {100} facets: In a typical synthesis, $Ce(NO_3)_3{\cdot}6H_2O$ (0.217 g, 0.05 mmol), oleic acid (1.10 mL) and 1.00 M TMAH aqueous solution (1.20 mL) were successively added to the mixture of 2.7 ml ethanol and 2 ml distilled water under intense ultrasonic treatment. The resulting solution was transferred to a Teflon-lined stainless steel autoclave (25 mL) and kept at 200 °C for 18 h. The products were collected by centrifugation at 10000 rpm, and washed several times with cyclohexane and ethanol.

2.2. Synthesis of truncated octahedral CeO_2 enclosed by {111} and {100} facets: In a typical synthesis, $Ce(NO_3)_3{\cdot}6H_2O$ (0.217 g, 0.05 mmol), 1.00 M TMAH aqueous solution (0.20 mL) and PVP (0.315 g, 0.006 mmol) were successively added to the mixture of 3 ml ethanol and 2.8 ml distilled water under intense ultrasonic treatment. The resulting solution was transferred to a Teflon-lined stainless steel autoclave (25 mL) and kept at 200 °C for 18 h. The products were collected by centrifugation at 10000 rpm, and washed several times with ethanol.

3. Characterization and measurements.

3.1. Characterization of morphology and structure: The composition and phase of as-prepared products were acquired by the powder X-ray diffraction (XRD) pattern, recorded on a Panalytical X-pert diffractometer with Cu-Ka radiation. The morphology and crystal structure of the as-prepared products were observed by scanning electron microscopy (SEM, S4800) and high-resolution transmission electron microscopy (HRTEM, JEM 2100) with an acceleration voltage of 200 kV. All TEM samples were prepared by depositing a drop of

diluted suspension in distilled water on a copper grid coated with carbon film. The surface compositions of CeO_2 samples were determined by a PHI QUANTUM2000 photoelectron spectrometer (XPS) using a monochromatic magnesium X-ray source. The binding energies were calibrated with respect to the signal for adventitious carbon (binding energy of 284.6 eV). Fourier transform IR (FTIR) spectra were collected with a Nicolet AVATAR 330 FTIR spectrophotometer. Raman spectra were recorded at ambient temperature with a 532 nm laser excitation on a Horiba Xplora Raman Spectrometer and the laser power on the sample was 4 mW. The surface areas (S) of the two types of CeO_2 nanoparticles were measured by the Brunauer-Emmett-Teller (BET) method by measuring nitrogen adsorption and desorption isotherms on a Micrometrics ASAP 2020 system.

3.2. Measurement of catalytic CO oxidation:

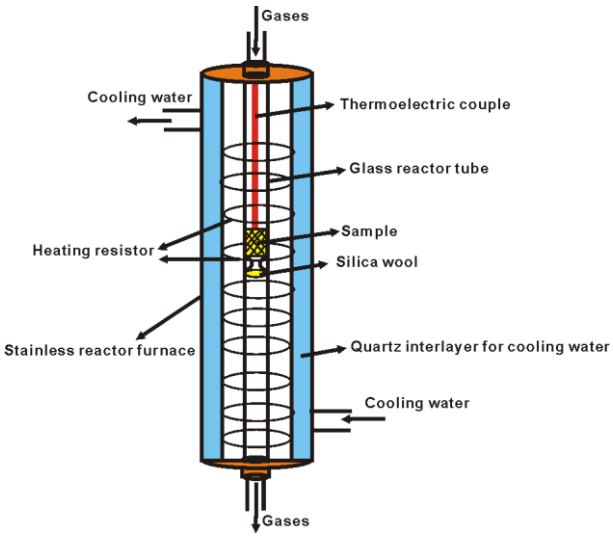

Scheme S1. The schematic drawing of the catalytic reactor setup used in the experiment.

Scheme S1 shows the catalytic reactor setup used in the experiment. Before the measurement, the CeO_2 catalysts were annealed at 400 °C for 2h. The catalytic activity of CeO_2 catalysts towards CO oxidation was carried out in a continuous flow reactor. The reaction gas, 5% CO in nitrogen (99.999% purity) (10 $mLmin^{-1}$) and air (99.999% purity) (40 $mLmin^{-1}$) was fed to catalyst nanoparticles (0.10 g) which was set in a fixed-bed flow reactor made of glass with an inner diameter of 2.4 mm. Steady-state catalytic activity was measured at each temperature, with the reaction temperature rising from room temperature to 280 °C in step of 20 °C. The effluent gas was analyzed on-line by an on-stream gas chromatograph (Ramiin GC 2060) equipped with a TDX-01 column.

Table S1 The BET specific surface areas of two types of CeO_2 particles.

Samples	BET surface areas (m^2g^{-1})
Cubic CeO_2{100}	57.72
Truncated octahedral CeO_2 {100}+{111}	40.63

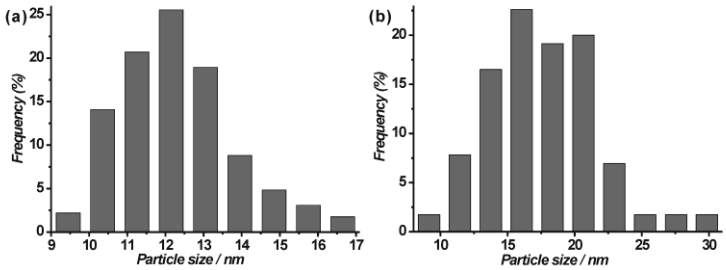

Fig. S1 The histogram of particle size distributions of the CeO_2 nanocrystals: (a) cubic CeO_2; (b) truncated octahedral CeO_2.

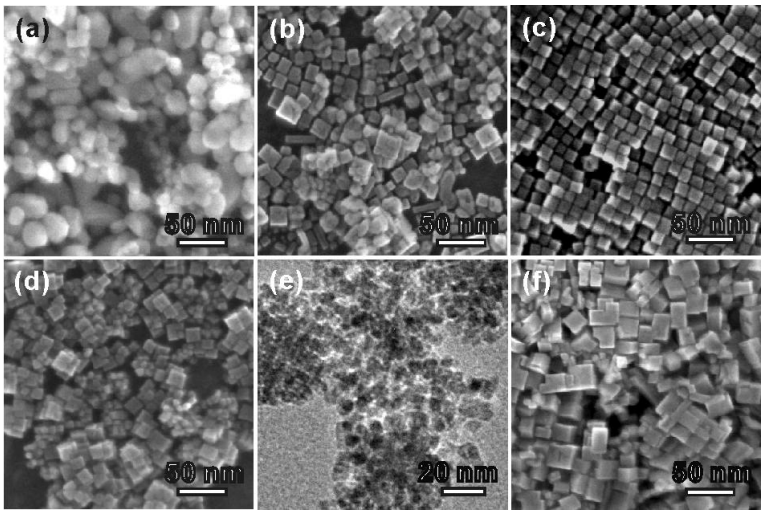

Fig. S2 SEM and TEM images of CeO_2 nanoparticles synthesized with different volume of oleic acid or TMAH: 0.0 ml (a), 0.2 ml (b), 1.1 ml (c), 2.5 ml (d) oleic acid and 1.20 mL TMAH in a total 7.0 ml growth solution; 0.1 ml (e), 3.2 ml (f) TMAH and 1.1 ml oleic acid in a total 7.0 ml growth solution.

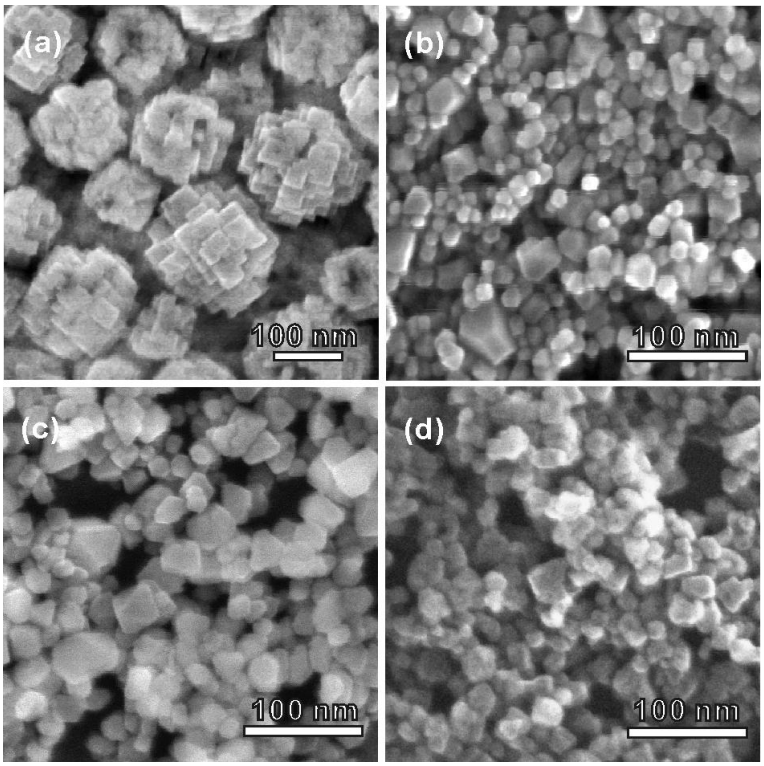

Fig. S3 SEM images of CeO_2 nanoparticles synthesized with different volume of TMAH or different mass of PVP: 0.0 ml (a) and 0.8 ml (b) TMAH in 6.0 ml growth solution; 0.0 g (c) and 0.47 g (d) in 6.0 ml growth solution.

Appropriate TMAH and PVP was essential in the formation of CeO_2 truncated octahedra. Without TMAH, CeO_2 flowers assembled by particles have been obtained (Fig. S3a). When the amount of TMAH was increased to 0.8 mL, truncated octahedra with different diameters ranging from 10-70 nm have been formed in the products (Fig. S3b). On the other hand, when no PVP is added, a few truncated octahedra can be obtained and the other particles are irregular (Fig. S3c). However, with excess PVP added, the obtained products are also irregular (Fig. S3d). In this case, appropriate TMAH provide a suitable growth environment, while the PVP was used as an capping agent to contol the morphology of CeO_2. Therefore, it is reasonable that the capping agents and an appropriate alkaline environment is essential for the formation the CeO_2 nanocubes and truncated octahedra.

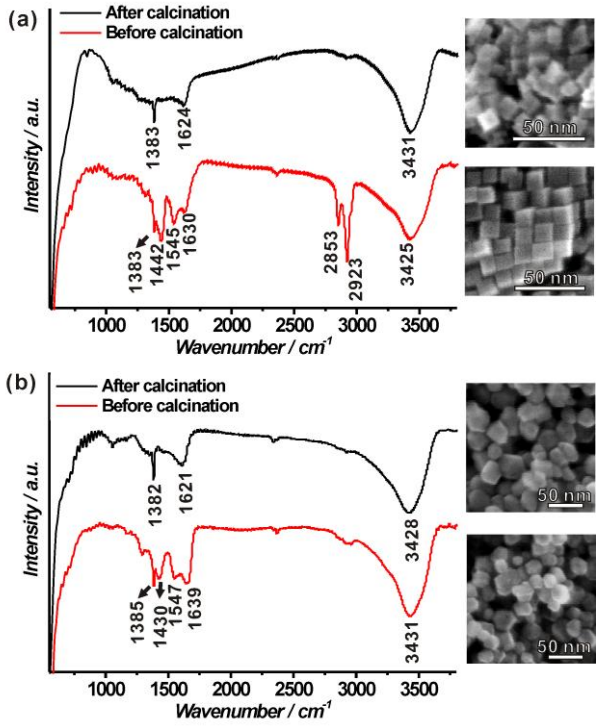

Fig. S4 FTIR spectra of CeO_2 nanocrystals before calcination and after calcination: (a) cubic CeO_2, (b) truncated octahedral CeO_2. Inset: SEM images of the CeO_2 particles before calcination and after calcination.

As shown in Fig. S4a, before calcination, the doublet at 2853 and 2923 cm^{-1} indicated the C-H stretching mode of methyl and methylene groups. The bands at 1442 and 1545 cm^{-1} represented the stretching frequency of the carboxylate group, which indicated that the carboxylate group in oleic acid chemically bonded with the Ce ions on the surface of CeO_2 nanocrystals.[1-4] However, these bonds disappeared after calcination, indicating the almost removal of the oleic acid. Similarly, as shown in Fig. S4b, before calcinations, the bands at 2853, 2923 cm^{-1} indicated the C-H stretching mode of methyl and methylene groups. The bands at 1430 and 1547 cm^{-1} represented the stretching vibrations of -C=O of PVP.[5] These bonds disappeared after calcination indicating the almost removal of the PVP. It should be pointed that the shapes of the CeO_2 nanocrystals were well kept during the annealing as showed in the inset of Fig. S4.

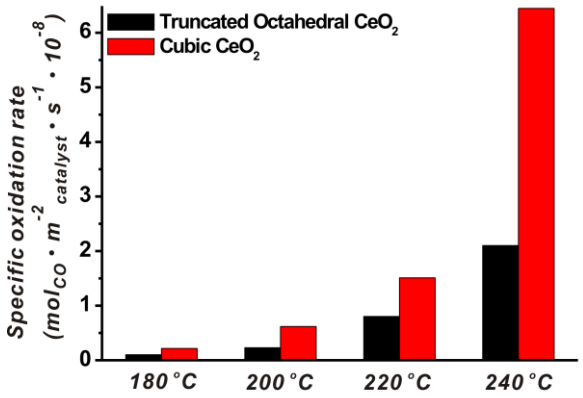

Fig. S5 Specific oxidation rates of CO over two types of CeO_2 nanocrystals at different temperatures.

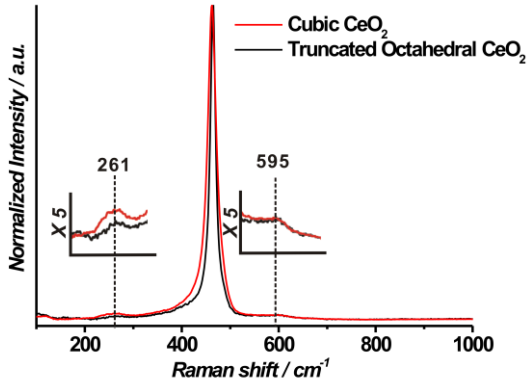

Fig. S6 Normalized Raman spectra of annealed CeO_2 nanocrystals. Inset: An enlarged view of the section around 261 cm^{-1} and 595 cm^{-1}.

As shown in Fig. S7, the highest intense peak at 464 cm^{-1} was the Raman active F_{2g} mode of CeO_2, which is due to symmetrical stretching mode of Ce-O8 vibrational unit.[6] Besides, two other low intense peaks at 261 cm^{-1} and 595 cm^{-1} appear on high and low energy sides of F_{2g} peak, indicating the existence of the O^{2-} vacancy in the annealed CeO_2 nanocrystals.[7,8] The stronger intensity of the peak around 261 cm^{-1} and the broad F_{2g} peak suggested that there are more coordination unsaturated cerium atoms (such as CeO_{2-x}) in the nanocubes than that in the truncated octahedra.

References:

1. J. Zhang, S. Ohara, M. Umetsu, T. Naka, Y. Hatakeyama, T. Adschiri, *Adv. Mater.*, 2007, **19**, 203.
2. F. Dang, K. Kato, H. Imai, S. Wada, H. Haneda , M. Kuwabara, *Cryst. Growth Des.*, 2010, **10**, 4537.
3. Y. G. Aronoff, B. Chen, G. Lu, C. Seto, J. Schwartz, S. L. Bernasek, *J. Am. Chem. Soc.*, 1997, **119**, 259.
4. C. Binet, M. Daturi, *Catal. Today*, 2001, **70**, 115.

5. C. Zhao, A. Zhang, Y. Zheng, J. Luan, *Mater. Res. Bull.*, 2012, **47**, 217.

6. T. Suzuki, I. Kosacki, H.U. Anderson, P. Colomban, *J. Am. Ceram. Soc.*, 2001, **84**, 2007.

7. Z. V. Popovic, Z. Dohcevic-Mitrovic, M. J. Konstantinovic, M. Scepanovic, *J. Raman Spectrosc.*, 2007, **38**, 750.

8. B. Choudhury, A. Choudhury, *Mater. Chem. Phys.*, 2012, **131**, 666.